Several Numerical Schemes for the Computation of Unsteady Flow in Pulsed Lasers

B. N. Srivastava,* G. Waldman,† J. Cruickshank,‡ and J. Moran‡
Avco Research Laboratory, Inc., Everett, Massachusetts

This paper describes numerical formulation issues aimed at developing an accurate computational approach for two-dimensional acoustic studies in a typical pulsed laser system. This goal is achieved through a series of numerical algorithm studies, optimizations thereof, and improved boundary formulation techniques related to the complex laser system environment. Several model test problems are computed and successfully compared with available data/analyses to demonstrate the accuracy of the computational approach.

Nomenclature

a = acoustic speed
C_d = discharge coefficient
e = specific internal energy
k_r = muffler wall resistance
M = Mach number
p = pressure
u = x component of velocity
v = y component of velocity
α = open area ratio for muffler wall
γ = ratio of specific heats
λ = laser light wavelength
ρ = density

Subscripts

c = channel side of muffler wall
m = muffler side of muffler wall
h = related to muffler hole properties
t = partial derivative relative to time
x = partial derivative relative to x coordinate
y = partial derivative relative to y coordinate

I. Introduction

In a high rep rate pulsed laser cavity, necessary requirements for obtaining high quality output laser beams are the efficient removal of waste heat and the effective damping of acoustic disturbances during the intrapulse time. These waves are generated in the laser cavity during the laser pumping process and are basically caused by the waste heat part of the total energy deposited in the laser cavity. The strength and nature of these waves depend on several parameters which are generally characteristics of an individual laser system. In general, two types of acoustic waves are generated in a laser cavity. The longitudinal acoustic waves (i.e., in the flow direction) are generated because the energy deposition to achieve laser pumping takes place in a small confined zone.[1] Almost invariably, this energy deposition time is very short compared to the acoustic transit time across the cavity. This, therefore, results in an overpressure of the pumped region, causing longitudinal waves. These waves have been addressed in several recent investigations for CO_2,[2] chemical,[3,4] and excimer[5-8] lasers. Waves moving predominantly transverse[9,10] to the flow direction are caused by two reasons:

1) The nonuniform energy deposition transverse to the flow.[1] This mechanism of transverse wave generation is generally not important because any significant nonuniformity in the energy deposition can be avoided by proper choice of design variables of the laser cavity.[1] Nonetheless, in some laser systems, such as an excimer laser,[9] this effect may remain significant because the output laser wavelength is small ($\lambda < 0.5$ μm), implying a more stringent medium homogeneity requirement.

2) In some laser systems (such as in a CO_2 Electric Discharge Laser), the electrodes are slightly displaced from the sidewalls,[1] preventing an arc from piercing the electron-beam foil. This results in almost no energy deposition between the foil and the electrode rod, giving rise to strong transverse waves. Thus, a system like this would consist of strong longitudinal as well as transverse waves. In the presence of several other system components, addressing general acoustic decay behavior is a complex problem for which proper technical attention is required.

There have been several attempts in the past to address the decay behavior of longitudinal waves in a typical laser system.[2-9] Progress to address transverse wave issues has been very limited[9-11] due to the complexity of the problem involved. Analytical methods[9,10] have provided trend behavior in the past, but their range of validity and applicability for a complex laser environment is not understood. Thus, there is a need for further work in this area. Recent advances in computational methods offer an attractive means to address this problem. For this, a two-dimensional unsteady inviscid computational approach with appropriate accuracy for nonlinear (strong shocks, contacts, expansions, and their mutual interactions) as well as linear regimes is required. This paper identifies numerical approaches which can adequately deal with this complex problem. Several numerical schemes are evaluated using model problems which are representative of laser applications. Based on these studies, a promising numerical scheme and relevant boundary approaches are discussed. This effort is considered to be an initial step in establishing a computational approach for studying acoustic performance of a typical laser system.

This paper is divided into several sections. Section II outlines the physical problem and the relevant theoretical model. Section III deals with various numerical issues related to the integration of the conservation equations. Section IV

Presented as Paper 86-1076 at the AIAA/ASME Fourth Fluid Mechanics, Plasma Dynamics and Lasers Conference, Atlanta, GA, May 12-14, 1986; received May 20, 1986; revision submitted Oct. 15, 1986. Copyright © American Institute of Aeronautics and Astronautics, Inc., 1986. All rights reserved.

*Principal Research Scientist. Member AIAA.
†Scientist, Avco Systems Division, Wilmington, MA.
‡Principal Research Scientist.

deals with the application of several different numerical schemes to a simple laser related problem in an effort to assess their performance. Section V deals with ways of further improving the chosen algorithm relative to various boundary approaches. Section VI depicts examples of some studies which were conducted using the improved version of the computational approach. Finally, Sec. VII outlines the relevant conclusions which were derived from these studies.

II. Physical Problem and Theoretical Model

It is highly relevant to first understand the physics of the problem at hand. Figure 1 shows a typical near cavity laser system consisting of a cavity of length L, which is preceded by a muffler of length L_1 and depth h_1, and is followed by a muffler of length L_2 and depth h_2. It is sufficient to consider near cavity components since they dictate the acoustic damping procedure. Also shown in the figure are typical longitudinal and transverse energy deposition profiles[7] which contribute to longitudinal and transverse waves, respectively.

The theoretical model for the problem outlined previously is similar to prior modeling efforts.[2-5] The channel equations are two-dimensional Euler equations. Written in rectangular coordinates (x, y), they are

$$\rho_t + (\rho u)_x + (\rho v)_y = 0$$

$$\rho u_t + \rho u u_x + \rho v u_y + p_x = 0$$

$$\rho v_t + \rho u v_x + \rho v v_y + p_y = 0$$

$$\rho e_t + \rho u e_x + \rho v e_y + p(u_x + v_y) = 0$$

$$p = (\gamma - 1)\rho e \tag{1}$$

Equations (1) are only the basic equations and are solved in various forms using a coordinate transformation.

The muffler model is typically a time-dependent set of equations. They are obtained by spatially averaging the one-dimensional equations (no variation in the x direction is considered consistent with closely spaced baffle approximation[2]) using a linear velocity profile in the direction from the near channel muffler wall to the muffler backwall. The advantage of using this simplified model is the appropriate savings in the computational cost. In many ways this model is similar to our previous model, which was used in the one-dimensional flow code, and has been extensively tested in the past.[2,7,13]

The muffler wall is treated by a quasi-steady model for flow through orifices (similar to those in Refs. 2, 7, 12, and 13). These equations are

$$m = \alpha \rho_h v_h \tag{2}$$

Outflow:

$$M_h = \min\left\{\left[\frac{2}{\gamma-1}\left(\frac{p_c}{p_m}\right)^{(\gamma-1)/\gamma} - 1\right]^{1/2}, 1\right\}$$

$$\rho_h v_h = C_d\left[(\gamma p_c M_h)\Big/ a_c\left(1 + \frac{\gamma-1}{2} M_h^2\right)^{(\gamma+1)/2(\gamma-1)}\right] \tag{3}$$

Inflow:

$$M_h = \min\left\{\left[\frac{2}{\gamma-1}\left(\frac{p_m}{p_c}\right)^{(\gamma-1)/\gamma} - 1\right]^{1/2}, 1\right\}$$

$$\rho_h v_h = C_d\left[(\gamma p_m M_h)\Big/ a_m\left(1 + \frac{\gamma-1}{2} M_h^2\right)^{(\gamma+1)/2(\gamma-1)}\right] \tag{4}$$

where C_d is the discharge coefficient (~ 0.6). Subscript c refers to the channel side of the perforated wall, m the muffler side of the wall, and h the properties in the hole. A thin porous mat placed over the perforated plate, separating the channel and the muffler, can be simulated by replacing p_c with $p_c + k_r v_h$ in the above equations. Here, coefficient k_r is utilized to characterize a linear loss term in the wall perforations.

It can be shown that for small Δp, Eq. (2) can be reduced to the appropriate loss form (follows from a series expansion

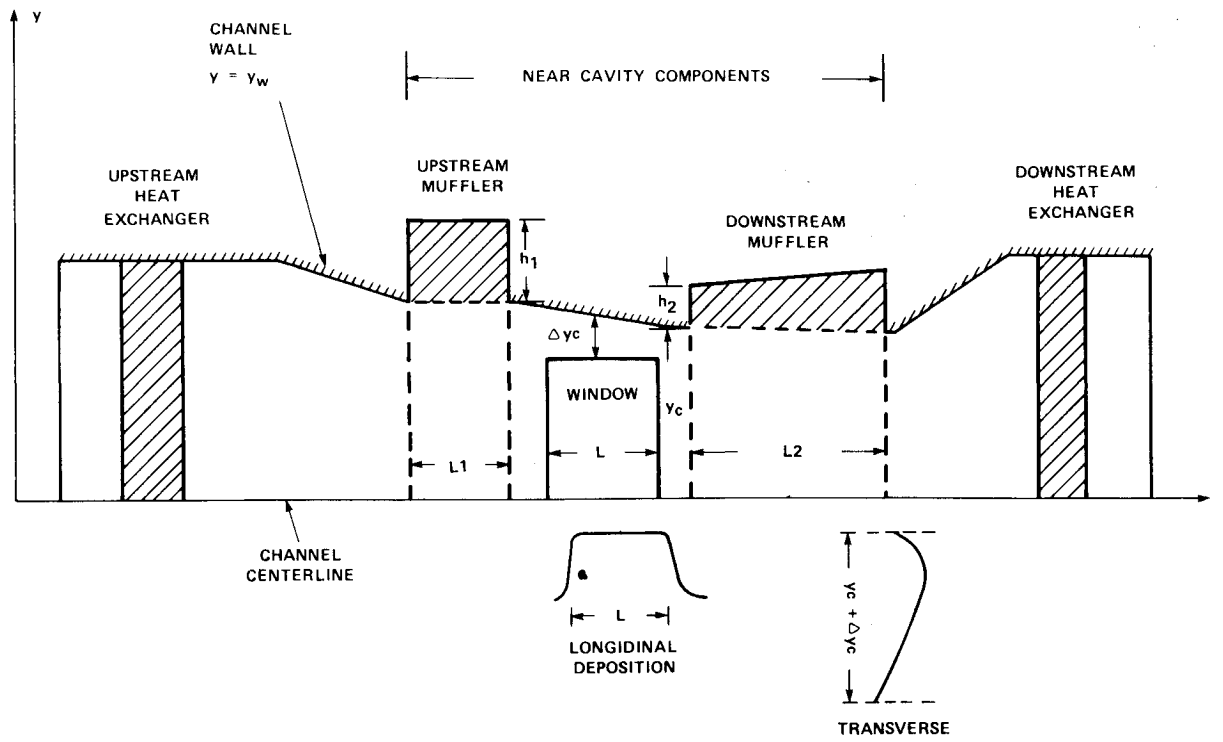

Fig. 1 Flow components of a typical pulsed laser.

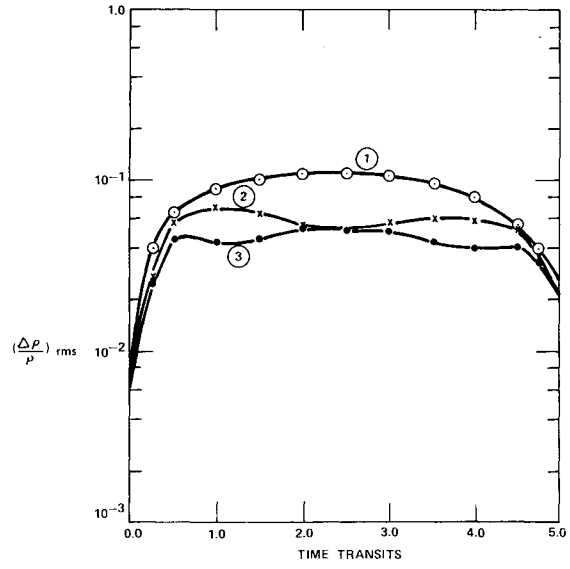

Fig. 2 Density perturbations clearing for the convection of a hot slug of gas in a constant area duct. Combination of MacCormack's scheme and characteristics update procedure. Curve labels are: (1) without optical correction; (2) with linear correction; (3) with quadratic correction.

for low Δp)

$$\Delta p \sim \rho_h v_h |v_h| / 2C_d + k_r v_h \tag{5}$$

Thus muffler wall is typically characterized by a linear and nonlinear loss term. Similar loss terms are included in the backing volume model.

The transport of momentum and energy for outflow/inflow follows from quasi-steady flow through orifices. For details of this, the reader is referred to Ref. 2, where all relevant equations are described.

III. Numerical Accuracy Issues

The computational analysis of the components shown in Fig. 1 demands a careful development for accurate acoustic predictions. There are many sources of numerical error that can contaminate the solutions for such devices. Our effort in identifying such sources of numerical error has led us to the following.

Aliasing Error

Energy deposition profiles in a typical laser cavity lead to shocks, expansions, and contact interfaces which are typically represented by large numbers of frequency components. Finite grid representation of such flow discontinuities cannot resolve all frequencies. Thus, to preserve total energy, spurious high-frequency components appear as wiggles (purely numerical). These wiggles can destroy the overall accuracy of the results.

To eliminate such numerical problems (for a practical problem on a reasonable grid size), two general classes of numerical schemes have been proposed. One class consists of such implicit damping procedures as λ schemes,[14] TVD schemes,[15] and FCT schemes.[16] These schemes are based on a blend of a lower order and higher order scheme. In general, a lower order dissipative weighting is utilized to eliminate the spurious oscillations typical of a higher order scheme. Such a scheme is monotone in nature. The other class of schemes belongs to explicit damping procedures. Typical of these schemes are those of MacCormack,[17] Jameson,[18] and Beam and Warming.[19] The latter procedures have been at times projected as variations of the implicit type,[20] implying that they can be shown to be equivalent to implicit types.

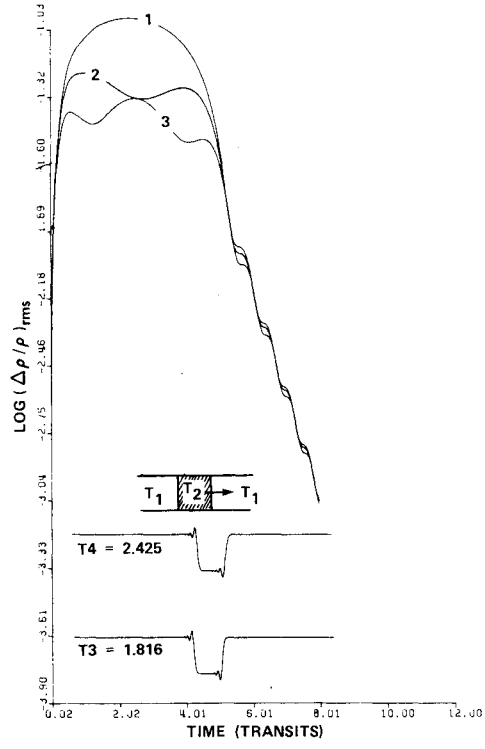

Fig. 3 MacCormack's scheme with a combination of second and fourth difference smoothing procedure. Density perturbations (top) and density pulse shape (bottom) are shown. Curve labels are the same as in Fig. 2.

A scheme based on fitting the discontinuities has no spurious numerical errors. Our one-dimensional code[2] is based on a fitting procedure, allowing for highly accurate computations. However, the coding effort for this procedure is complex and its extension to two-dimensions is very cumbersome. Thus, in two-dimensions, a scheme equivalent (in accuracy) to the discontinuity fitting scheme is highly desirable. We have performed several numerical tests using various schemes for a typical laser related problem to assess their accuracy of predictions. The results are discussed in Sec. V of this paper.

Geometric Error

Abrupt geometrical changes cause numerical errors. This form of error generation depends on the nature of the geometry being computed. In general, such abrupt geometrical changes imply discontinuous derivatives,[21] and thus, a Taylor's series expansion is not valid across it.[2,22] An appropriate local grid clustering or a local characteristics update is required to address this source of error. A local characteristics update works well because characteristics can accommodate discontinuous derivatives without creating any numerical error. As will be discussed in Sec. V, this source of error in our chosen two-dimensional algorithm was alleviated by a local characteristics update procedure.

Consistency Error

This is related to the consistency of numerical integration between the backing volume and the main channel. The integration of the backing volume equations must be consistent with that of the channel equations to achieve a late time pressure equilibration process. When muffler volume fills, the backing pressure and channel pressure equilibrate, and then inflow into the channel can occur. However, if significantly different errors are associated with the update procedures on two sides of the muffler wall, the equilibration process may not be acheived since there is no mutually

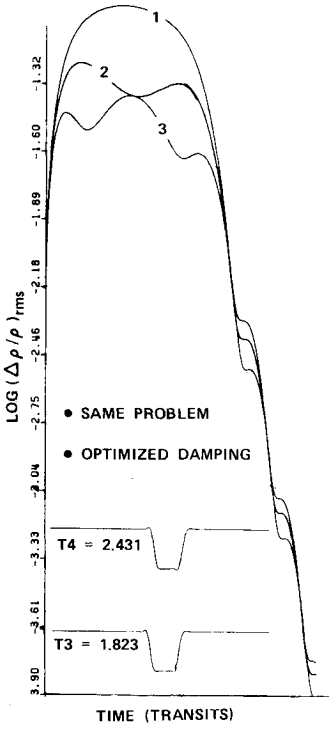

Fig. 4 MacCormack's scheme: optimized damping coefficients utilized. Density perturbations (top) and density pulse shape (bottom) are shown. Curve labels are same as in Fig. 2.

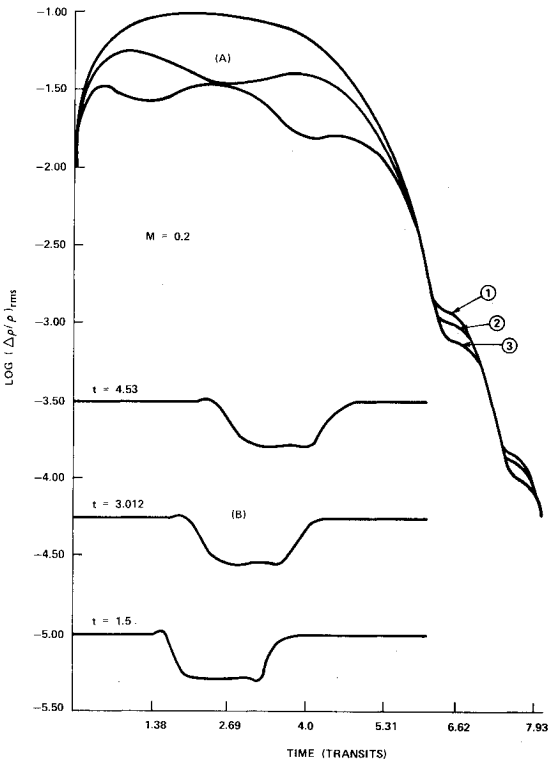

Fig. 5 Three point implicit scheme of Beam and Warming with smoothing: a) density perturbations; b) pulse shape. Curve labels are same as in Fig. 2.

acceptable equal pressure. It typically shows up as numerical oscillations when pressures on the two sides tend to equilibrate. Note, however, that in an implicit procedure where local variables on both sides of the muffler wall are simultaneously inverted and iterated upon, this problem does not arise. This is because the error is distributed to all variables, eliminating any consistency limitation. Convergence problem during an iterative procedure can, however, be encountered due to the truncation errors associated with computation of small mass flux. This problem typically arises in the absence of the linear term in Eq. (5). It is caused by the apparent square root singular behavior of the mass exchange process as Δp approaches zero. A heuristic scheme to alleviate this problem was implemented in our previous effort.[2]

Boundary Treatment Error

This source of numerical error relates to muffler wall treatment. Utilizing a reflection procedure[2] on the muffler wall in order to impose an appropriate mass flow through the wall was found to be highly erroneous. Numerical errors caused by this contaminated the flowfield and degraded the code performance. A local characteristic update procedure was found to eliminate this source of numerical error. Further discussion on this is given in Sec. V.

The present section outlines all the numerical accuracy issues we faced during our development effort. The following two sections are devoted to the actual numerical experiments that led us to these issues. We will discuss how we assessed these errors and what remedial action was taken to ensure that such problems were eliminated.

IV. Algorithm Considerations

We have investigated several aspects of the numerical accuracy issues for a given laser related problem in an effort to identify an appropriate numerical procedure with desired accuracy. In an effort to isolate the capability of a scheme, the sources of boundary errors were eliminated. This was done by considering a simple problem of propagation of a hot slug in a constant area duct. The following schemes were then evaluated on identical grid distributions:

1) Hybrid Explicit Scheme (combination of MacCormack's and characteristics[2]);

2) Explicit MacCormack's Scheme (with explicit dissipation[17]);

3) Implicit Beam and Warming Scheme (with explicit and implicit dissipation[19]); and

4) Flux Corrected Transport Algorithm—SHASTA (of Boris and Book.)[16]

Without going into the details of the numerical schemes (available in the references cited above), the results for these model problem studies are outlined next.

Figure 2 shows the result using scheme 1, where the discontinuities are fitted and tracked in time. At points away from such discontinuities, an explicit MacCormack scheme is used. Further details of this scheme are available in Refs. 2 and 13. The results of the numerical computations are presented in the form $(\Delta\rho/\rho)_{rms}$ over the cavity aperture. The other two curves represent linear and quadratic corrections. Notice from this figure that when the hot gas moves out of the active aperture, the density perturbations are totally eliminated. Thus, this scheme is performing with almost no numerical error—an ideal scheme. However, it cannot be easily extended to higher dimensions due to the complexity of the discontinuity fitting procedure.

Figure 3 shows the solution of the same problem using MacCormack's scheme[17,23] with Jameson's damping procedure.[18] Notice from this figure that the clearing process is dominated by spurious disturbances which tend to delay the clearing. In an effort to understand these results, a typical pulse profile (density profile) was plotted and is shown as an inset in Fig. 3. It is clear that the pulse shape is associated

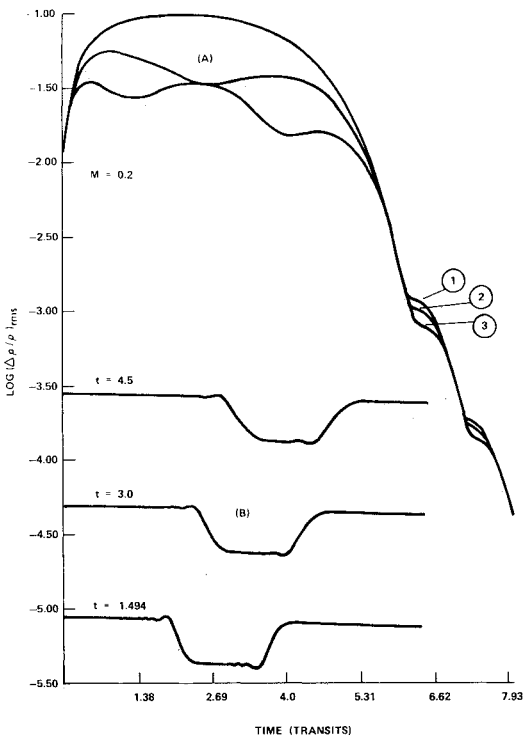

Fig. 6 Three point implicit scheme of Beam and Warming with Jameson's smoothing: a) density perturbations; b) pulse shape. Curve labels are same as in Fig. 2.

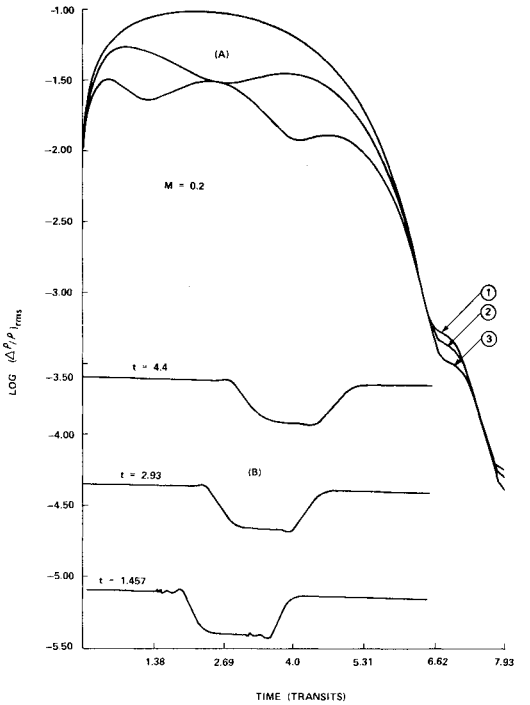

Fig. 7 Euler implicit scheme of Beam and Warming with Jameson's smoothing: a) density perturbations; b) pulse shape. Curve labels are same as in Fig. 2.

with oscillatory behavior which tends to delay the clearing process. To improve this situation, an optimization of the damping coefficients was undertaken. Figure 4 shows the same result with the optimized damping coefficients. An order of magnitude improvement in the clearing process is evident. The inset in Fig. 4 confirms that this improvement is attributable to the reduction of spurious oscillations associated with the discontinuities. In spite of the optimization, the results indicate significant density contamination (due to spurious oscillations) when compared with the results of Fig. 2.

Next, the implicit scheme of Beam and Warming[19] was utilized to solve the same problem. In an effort to obtain results using various forms of the scheme (with variation in damping terms), the following were obtained:

1) The three-point implicit scheme of Beam and Warming[19] was applied with two different smoothing procedures. The original method of Beam and Warming[19] applied with a second order implicit damping (on the left side of conservation equations) and a fourth-order explicit damping term (on the right side of conservation equations) was first attempted. Figure 5a shows the result when the implicit smoothing coefficient (μ_i) of 3.0 and explicit smoothing coefficient (μ_e) of 1.0 was chosen. The result shows a clearing process similar to the previous scheme using optimized coefficients. A study of the pulse behavior suggests (Fig. 5b) few oscillations, but some smearing of the pulse shape is fairly evident. The three-point implicit scheme of Beam and Warming was then applied with the smoothing procedure of Jameson.[18] Figure 6a shows the clearing process, and Fig. 6b shows the pulse shape. The clearing process and pulse shape are similar to those that were shown in Fig. 5. No additional advantage is observed by changing the damping procedure.

2) The Euler implicit scheme of Beam and Warming[19] was then utilized with Jameson's type of smoothing. Figure 7a shows the clearing process, while Fig. 7b shows the pulse shape. No new improvements are seen using this new approach.

The flux corrected transport (FCT) algorithms were designed[16] to implicitly remove the spurious oscillations associated with sharp discontinuities. More recent schemes, such as TVD[15] and schemes based on characteristics (flux splitting[24]), achieve the same goal. We have used the original scheme of Boris and Book,[16] "SHASTA," for current studies, even though more advanced FCT algorithms[25] are now available. The algorithm (by its very structure) is more expensive than the other two discontinuity capturing algorithms outlined above. The test case, as outlined above, was slightly modified to save some computer cost, allowing us to conduct a large number of numerical experiments. The flow Mach number was changed from 0.2 to 0.3. The grid size, however, was kept identical.

Figure 8 shows the results of the computation. This figure shows the results for $(\Delta\rho/\rho)_{\text{rms}}$, as well as $(\Delta p/\gamma p)_{\text{rms}}$, which are representative of density and pressure perturbations, respectively. There are several interesting points to be noted here. Notice that the clearing process using this algorithm is better than that of schemes 2 and 3. However, while schemes 2 and 3 showed no perturbations in pressure (they are of the same order as the machine accuracy), this scheme shows significantly high pressure perturbations which dominate the clearing process after the hot gas clears the averaging aperture. Notice also from this figure that while the density profile is also somewhat contaminated, the contamination is much less severe than in schemes 2 and 3. The pulse density shape, shown as an inset in this figure, appears very smooth and sharp.

We have attempted to improve the original scheme to eliminate the pressure perturbation problem outlined previously. The origin of these spurious perturbations was traced to the flux blending scheme. Several numerical experiments were performed to modify the inherent flux blending scheme associated with the SHASTA algorithm. The first attempt was to complement the SHASTA algorithm with a filtering scheme of Jameson's type, i.e., a blend of the second and fourth difference schemes was utilized to filter spurious pressure perturbations. In Fig. 9, curves 1 and 2 represent the pressure and density perturbations after using

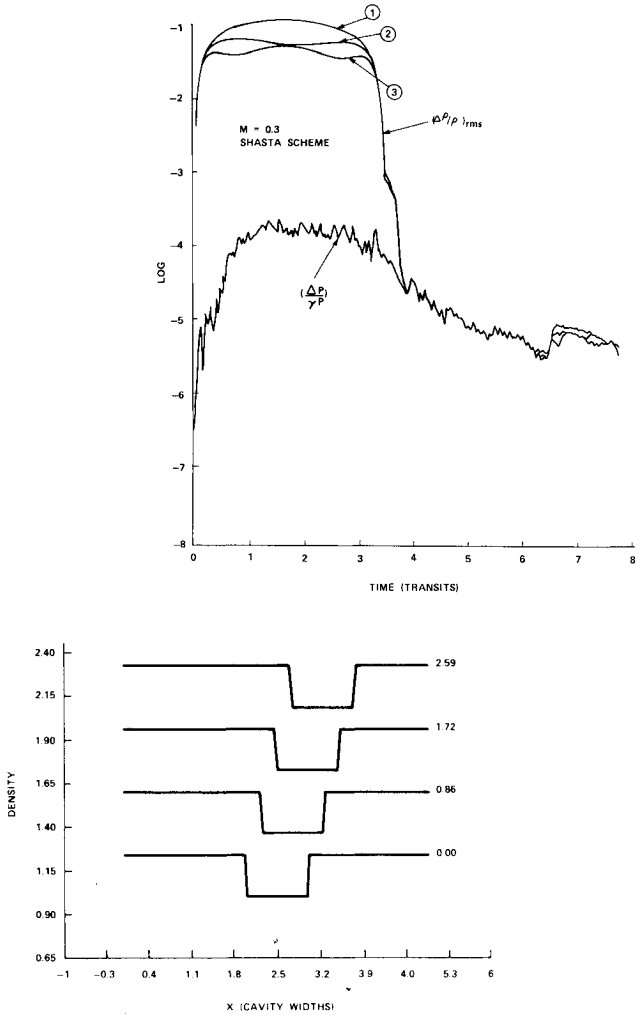

Fig. 8 Flux corrected transport algorithm—SHASTA. Notice the appearance of pressure perturbations created by the numerical scheme employed. Curve labels are same as in Fig. 2. Inset shows the density pulse shape.

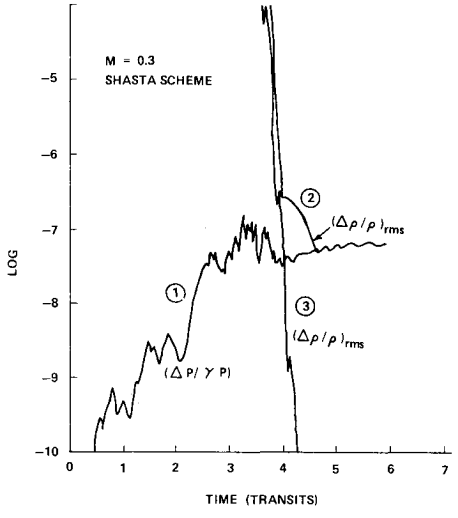

Fig. 9 Improved numerics utilized in SHASTA to eliminate spurious pressure perturbations. Curves (1) and (2) are pressure and density perturbations after using a Jameson's type filtering procedure; curve (3) shows results after modifying the flux blending scheme of SHASTA.

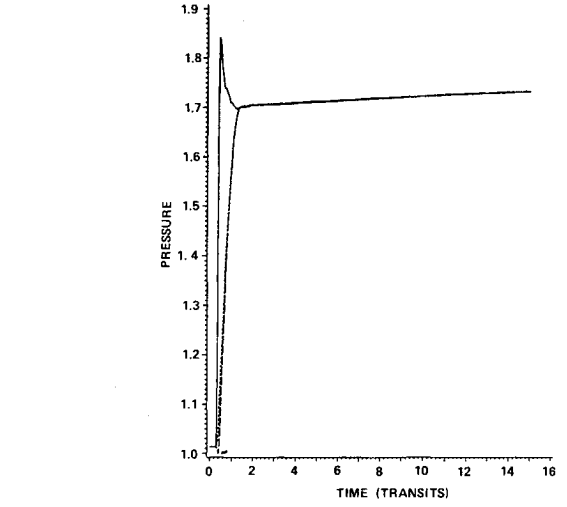

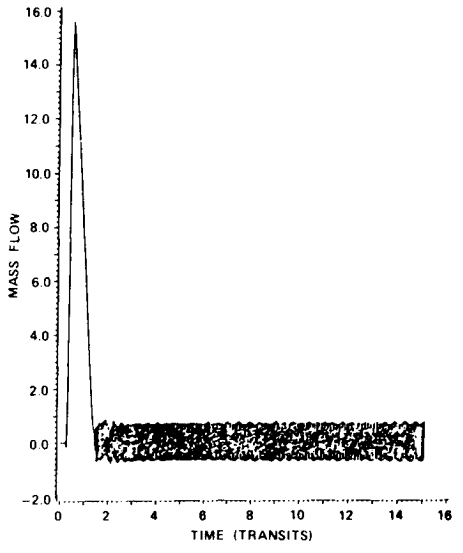

Fig. 10 Passage of an isolated shock through a duct with wall mufflers. Demonstration of numerical consistency error associated with the wall muffler update procedure. Channel and backing volume pressures and mass flux variations with time showing numerical oscillations. One-dimensional code was employed for this computation.

such a scheme. In comparison to Fig. 8, notice that while the pressure perturbations have decreased by two orders of magnitude, they have not been eliminated. The accuracy level of the scheme is of the order of 10^{-7} for this problem.

In an effort to determine whether further improvements are possible, we also experimented with the original flux blending scheme. In the original scheme, each conservative equation is blended separately. Figure 9, curve 3 shows the computational results when the flux blending in momentum and energy equations were made proportional to those in the continuity equation. As is observed from curve 3, the pressure perturbations were completely eliminated using this procedure. This represents a significant improvement in the algorithm for such computations.

The studies conducted indicate that the best performing algorithm, from an accuracy standpoint, is either a characteristics fitting procedure or an FCT algorithm. In one-dimension, coding of a characteristics approach is manageable, and, in the past, such a code has been successfully developed.[2,13] In higher dimensions, it suffers from extreme coding complexity. An FCT algorithm like SHASTA is computationally more expensive (~2 or more) than the currently

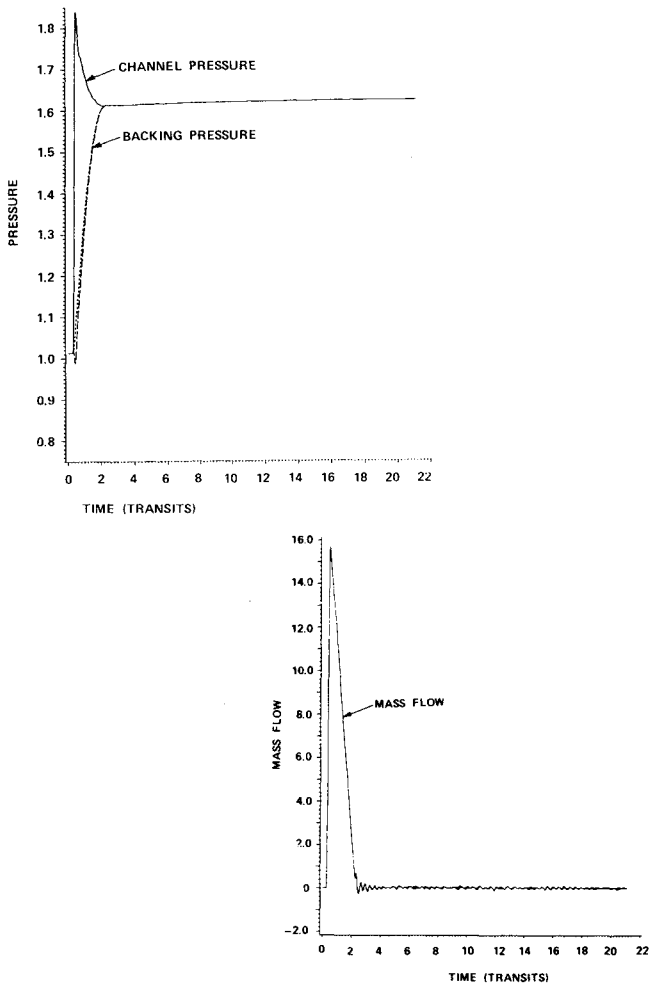

Fig. 11 Improved computational results (as compared to Fig. 10) after employing a first order integration procedure in the backing volume. Channel and backing volume pressures and mass flux variations with time shown. One-dimensional code was utilized.

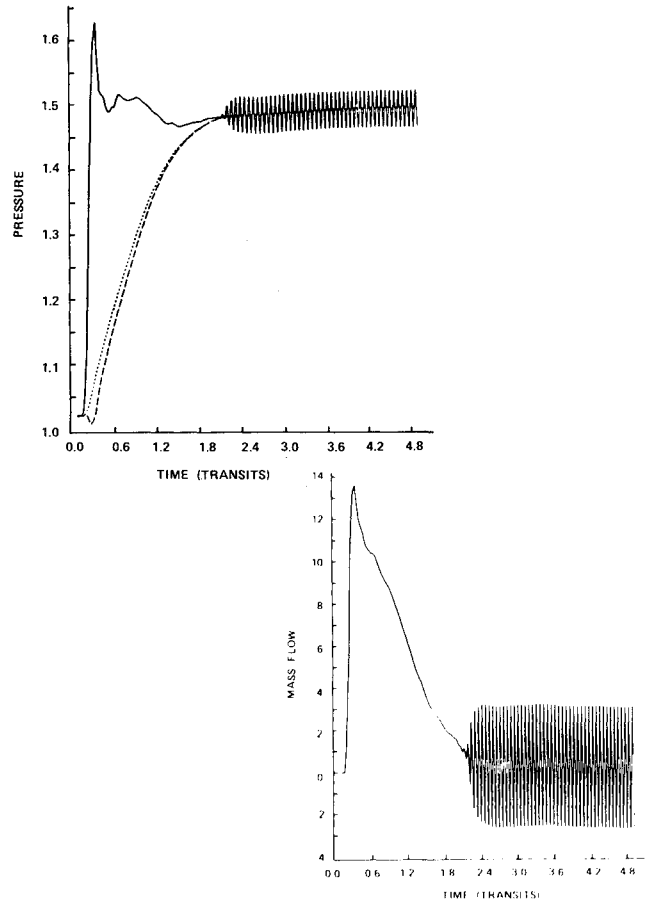

Fig. 12 Demonstrating muffler wall update error due to reflection treatment. Two-dimensional code was utilized. Channel and backing volume pressures and mass flux variations with time shown.

popular schemes 2 and 3. The accuracy requirement, however, for laser acoustic problems dictates its utilization for laser applications.

It must be further noted that algorithm considerations are only a first step toward developing an accurate computational approach for unsteady laser flow computations. The equally important boundary approach considerations, as outlined in Sec. III, are now addressed through more model problem studies (related to laser applications).

V. Model Problem Studies

In this section, model problems are utilized to first demonstrate a typical source of numerical error. Advanced numerical schemes are then developed to eliminate them. The details are described next. The numerical scheme used for all studies is the SHASTA algorithm.

One of the major sources of numerical error is the consistency error described in Sec. III. To illustrate this, we consider a one-dimensional problem rleated to the passage of an isolated one-dimensional shock through a finite capacity sidewall muffler (in some sense this problem is an ideal representation of a typical laser component). We have considered only the one-dimensional situation here in order to eliminate any numerical error associated with the wall boundary condition in a two-dimensional configuration. Figure 10 shows the pressure equilibration process between the backing volume of the muffler and the main channel at the inlet to the muffler. Nothing unusual appears in the results until one computes mass flux at the same location. An oscillatory behavior in mass flux (near pressure equilibration) is observed (see inset in Fig. 10). These oscillations are typically representative of the numerical consistency errors assoicated with the integration procedure on the two sides of the muffler wall. We considered several numerical experiments to eliminate this problem. Most of these experiments related to the variation of the integration procedure in the backing volume. A first order integration procedure was found to be highly successful. The results for the improved numerical scheme are shown in Fig. 11: notice that the mass flux oscillations are very effectively eliminated. This represents a substantial improvement in the overall scheme for such problems.

The first order integration scheme, as identified above, was used for the integration of the backing volume equations in the two-dimensional SHASTA code. In the two-dimensional code, only channel equations are solved in a two-dimensional sense, while backing volume equations are spatially averaged time dependent equations, as described in Sec. II. The two-dimensional code depicted an entirely new numerical problem as shown in Fig. 12. Figure 12 shows the pressure in the backing volume side and the channel side of the muffler wall. At late times, the wall channel pressure shows numerical oscillations. Note that this behavior is significantly different from that seen in Fig. 10 where large wall channel pressure oscillations were not observed. Figure 12 also shows the large mass flux oscillations caused by the wall channel pressure oscillations. A series of numerical experiments were then conducted to isolate the source of this error. It was found that this numerical error was caused by the reflection treatment at the muffler wall. This procedure tended to generate large numerical errors, contaminating the late time behavior. A local one-dimensional characteristics update procedure, normal to the muffler wall, that takes ap-

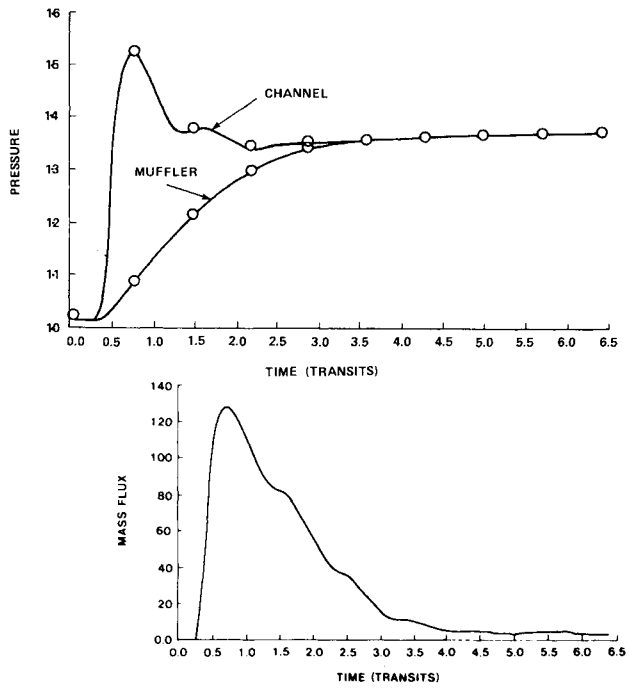

Fig. 13 Improved computational results using characteristics update for muffler wall boundary condition. Pressure and mass flux variations shown.

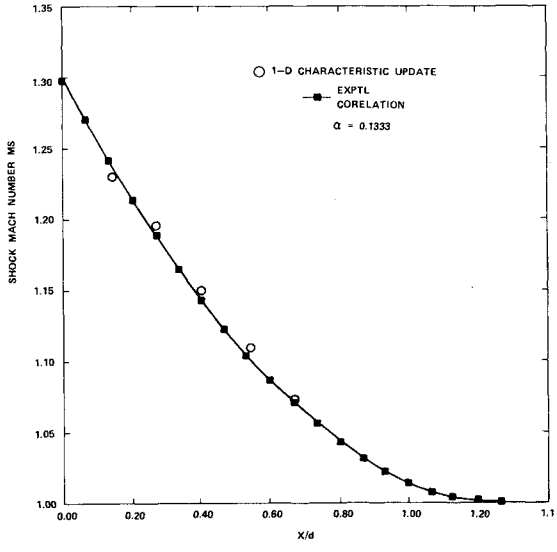

Fig. 14 Comparison of computational results with experimental correlation for passage of an isolated shock through a circular duct with infinite capacity wall muffler.

propriately correct characteristic information for inflow and outflow was utilized to advance the conservation variables at the muffler wall. This procedure is iterative and is implemented at the end of each time step. This scheme was found to be successful in eliminating the numerical problem associated with the implementation of the muffler wall boundary condition. The results are shown in Fig. 13 for the pressure and mass flux. Notice that the oscillations seen in Fig. 12 have been totally eliminated.

A series of tests were then conducted to evaluate the two-dimensional code performance. Test cases for which experimental data and other theoretical calculations were available were used. Figure 14 shows the predicted decay behavior of the passage of an isolated shock through an infinite capacity muffler (using the improved two-dimensional SHASTA code), as compared to the experimental correlation.[2] The overall comparison between the predicted and experimental data is reasonably good. Figure 15 shows the shock decay in an area variation, as compared to linear theory of Chisnell.[26] The comparison between the two predictions is also reasonably good here. Figure 16 shows a comparison between the code predictions and linear theory[9] for a tilted side wall cavity configuration. The geometry and deposition profile is shown in Fig. 16. It is observed from this figure that the comparison between the two predictions for cavity clearing is reasonably good. Further comprehensive code tests, with currently undergoing experiments, are planned. The next section, however, describes some results using this code to demonstrate the nature of the predictions that can help in laser system design studies.

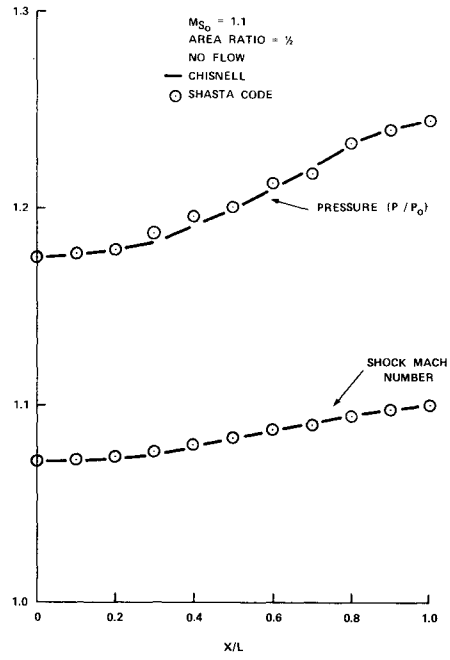

Fig. 15 Comparison of computational results with Chisnell's analysis for decay of an isolated shock in duct with increasing area.

VI. Laser Related Acoustic Studies

The prime motivation (and therefore the utility of the code described) of this paper relates to developing an understanding of the controlling design parameters which can effectively damp transverse waves in a laser cavity. In this section, we discuss specific studies which demonstrate the utility of such a design tool without resorting to a specific laser system.

Figure 17 shows the computational results obtained from an idealized hardwall duct laser cavity geometry with a uniform deposition in the transverse direction but with a longitudinal deposition profile as shown in Fig. 1. For this problem, the cavity clearing mechanism is the convection of hot gas zone from the laser cavity. As one would physically expect, and as is seen in this figure, the pressure perturbations are very rapidly cleared from the laser cavity in the absence of any reflection from nearby laser flow elements. Figure 17 also shows the computational results when the transverse deposition is made nonuniform (as shown in Fig. 1). Notice that the presence of transverse waves has a pronounced effect on the cavity clearing (curves a, in Fig. 17) process. The only decay mechanism for these transverse waves is through radiation, a decay process that is considered to be relatively slow (analytical predictions in linear regime suggests at $t^{-1/2}$ decay process). Notice also from this

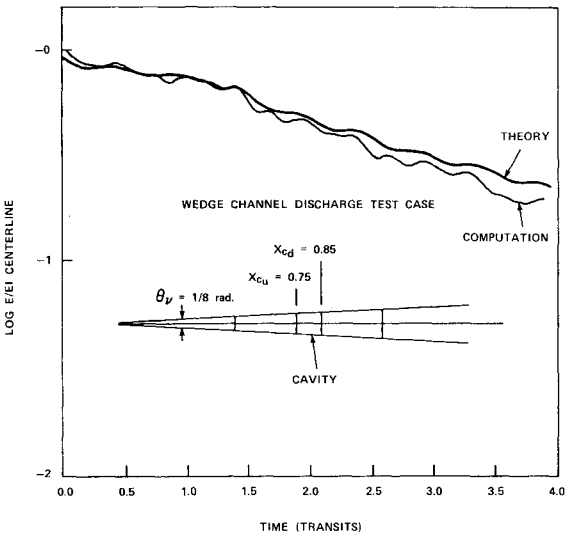

Fig. 16 Acoustic clearing as predicted by the present method compared to computed results of Ref. 9.

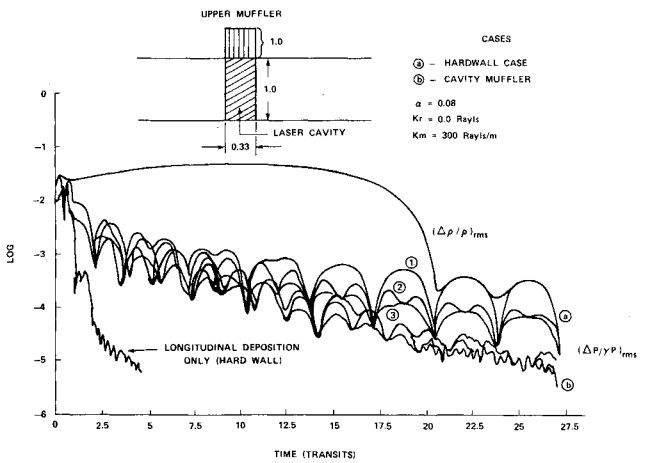

Fig. 17 Laser cavity acoustic clearing for an idealized laser system geometry. The clearing process is dominated by the presence of transverse waves. A sidewall muffler in the laser cavity results in an improved acoustic recovery process (curves b) as compared to a hardwall case (curves a).

figure that pressure perturbations (representative of acoustic waves) initially have a very large slope (indicating dominant longitudinal clearing) and then have a reduced slope (indicating slow transverse wave clearing). This decay behavior can be altered by employing suitably designed, carefully located acoustic attenuators in the laser flow system loop. We do not intend to address this general problem here, but show that this transverse wave decay pattern can be altered (affecting overall maximum pulse repetition frequency, PRF, and therefore overall system laser extracted power). Figure 17 also shows the computed results when a finite capacity sidewall muffler is placed over the cavity sidewall. The optimized parameters of the muffler used in this computation are also shown in this figure. It is evident that a much more rapid acoustic decay process (curves b, in Fig. 17) is observed, as compared to the hardwall case. The idealized test problems studied here tend to demonstrate the relevant dominant physics associated with the acoustic recovery process in a laser cavity, leading to the need to control design parameters. These studies will help in determining the choice of various parameters in full laser cavity configuration. Further studies in this area are planned in order to understand the overall design aspects.

VII. Conclusions

This paper represents a first step toward developing an accurate computational approach for two-dimensional acoustic studies in a typical pulsed laser system. Within the context of the adopted model, this paper describes in detail the relevant numerical aspects of simulating a complex laser system consisting of the laser cavity and the near cavity flow elements such as perforated wall and finite capacity sidewall muffler. A series of numerical studies and optimizations are first performed to assess the capability of various algorithms relevant to an idealized laser related problem. The optimized best performing algorithm (FCT-SHASTA scheme) is then applied to several other model problems. The deficiency in the numerical scheme (after such an application) is identified, and is subsequently remedied by developing improved numerical schemes. A series of test problems are then computed and compared with other available results. Computational studies are performed by simulating idealized laser configurations in an effort to develop an understanding of the decay behavior of laser generated pulses and the impact of some design parameters. The studies contained herein demonstrate that a carefully developed computational approach can yield highly accurate solutions, allowing useful design guides for laser applications.

Acknowledgment

This research work was sponsored by AFWL under Contract F29601-84-C-0091. The authors are indebted to the contracting agency for continued financial support in this area.

References

[1]Srivastava, B. N., Theophanis, G., Limpaecher, R., and Comly, J. C., "Flow and Discharge Characteristics of Electron-Beam-Controlled Pulsed Lasers," *AIAA Journal*, Vol. 19, July 1981, pp. 885-892.

[2]Srivastava, B. N., Knight, C. J., and Zappa, Q., "Acoustic Suppression in a Pulsed Laser System," *AIAA Journal*, Vol. 18, May 1980, pp. 555-562.

[3]Ausherman, D. R., Alber, I. E., and Baum, E., "Acoustic Suppression in Pulsed Chemical Laser," *AIAA Journal*, May 1979, pp. 490-497.

[4]Thayer, W. J. III, Buonadonna, V. R., and Sherman, W. D., "Pressure Wave Suppression for a Pulsed Chemical Laser," AIAA Paper 78-1216, July 1978.

[5]Hogge, H. D. and Crow, S. C., "Flow and Acoustics in Pulsed Excimer Lasers," presented at AIAA Conference on Fluid Dynamics of High Power Lasers, Oct.-Nov. 1978.

[6]Tong, K., Knight, C. J., Singh, P., and Srivastava, B., "Flow and Acoustics Study for Pulsed Visible Lasers," AIAA Paper 80-0348, Jan. 1980.

[7]Tong, K., Knight, C. J., and Srivastava, B., "Pressure Wave Attenuation in Mufflers with Finite Backing Volume," AIAA Paper 79-0602, March 1979.

[8]Schwartz, J., Kulkarny, V. A., and Ausherman, D. A., "Pressure Wave Attenuation in Repetitively Pulsed Fusion Lasers, 'Shock Tubes and Waves'," *12th International Symposium on Shock Tube and Waves*, Jerusalem, July 1979, Magnes Press, 1980.

[9]Knight, C. J., "Transverse Acoustic Waves in Pulsed Lasers," AIAA Paper 81-1283, June 1981.

[10]Kulkarny, V., "Decay of Transverse Acoustic Waves in a Pulsed Gas Laser," *AIAA Journal*, Nov. 1980, pp. 1336-1341.

[11]Morris, J., Levin, J., Crow, S., and Hurdle, P., "Further Investigations of Flow and Acoustics in Pulsed Excimer Laser," Poseidon Research Rept. 32, Santa Monica, CA, Aug. 1980.

[12]Beavers, G. S. and Sparrow, E. M., "Compressible Gas Flow through a Porous Material," *International Journal of Heat and Mass Transfer*, Vol. 14, 1971, pp. 1855-1859.

[13]Srivastava, B. N., "Pressure Wave Attenuation due to Anode Mufflers in Pulsed Lasers," *AIAA Journal*, Vol. 21, March 1983, pp. 381-389.

[14]Napolitano, M. and Dadone, A., "Three-Dimensional Implict Lambda Methods," Proceedings of the 5th GAMM Conference on Numerical Methods in Fluid Mechanics, Rome, Oct. 1983.

[15]Harten, A., "A Resolution Scheme for the Computation of Weak Solutions of Hyperbolic Conservation Laws," *Journal of Computational Physics*, Vol. 49, 1983, pp. 357-393.
[16]Boris, J. P. and Book, D. L., "Flux-Corrected Transport I, SHASTA—A Fluid Transport Algorithm that Works," *Journal of Computational Physics*, Vol. 11, 1973, p. 38 (also, Boris, J. P., "Flux Corrected Transport Modules for Solving Generalized Continuity Equations," NRL Memo 3237, March 1976).
[17]MacCormack, R. W., "The Effect of Viscosity in Hypervelocity Impact Cratering," AIAA Paper 69-354, 1969.
[18]Jameson, A., Schmidt, W., and Turkel, E., "Numerical Solutions of the Euler Equations by Finite Volume Methods Using Runge-Kutta Time-Stepping Schemes," AIAA Paper 81-1259, June 1981.
[19]Beam, R. M. and Warming, R. F., "An Implicit Factored Scheme for the Compressible Navier-Stokes Equations," *AIAA Journal*, Vol. 16, April 1978, pp. 393-402.
[20]Pulliam, T. H., "Artificial Dissipation Models for the Euler Equations," AIAA Paper 85-0438, Jan. 1985.
[21]Srivastava, B. N., Werle, M. J., and Davis, R. T., "A Finite Difference Technique Involving Discontinuous Derivatives," *Computers and Fluids*, Vol. 7, No. 1, March 1979, pp. 69-74.
[22]Roache, P. J., *Computational Fluid Dynamics*, Hermosa Publishers, Albuquerque, NM, 1972.
[23]Srivastava, B. N., "Computation of Flow Fields in High Solidity and High Turning Angle Cascades using Euler Equations," AIAA Paper 85-1705, July 1985.
[24]Steger, J. L. and Warming, R. F., "Flux Vector Splitting of the Inviscid Gas Dynamic Equations with Application to Finite-Difference Methods," *Journal of Computational Physics*, Vol. 11, 1973, p. 28.
[25]Zalesak, S. T., "Fully Multidimensional Flux Corrected Transport Algorithms for Fluids," *Journal of Computational Physics*, Vol. 31, 1979, p. 335.
[26]Chisnell, R. F., *Journal of Fluid Mechanics*, Vol. 2, 1957, p. 286.

From the AIAA Progress in Astronautics and Aeronautics Series...

COMBUSTION DIAGNOSTICS BY NONINTRUSIVE METHODS – v. 92

Edited by T.D. McCay, NASA Marshall Space Flight Center
and
J.A. Roux, The University of Mississippi

This recent Progress Series volume, treating combustion diagnostics by nonintrusive spectroscopic methods, focuses on current research and techniques finding broad acceptance as standard tools within the combustion and thermophysics research communities. This book gives a solid exposition of the state-of-the-art of two basic techniques—coherent antistokes Raman scattering (CARS) and laser-induced fluorescence (LIF)—and illustrates diagnostic capabilities in two application areas, particle and combustion diagnostics—the goals being to correctly diagnose gas and particle properties in the flowfields of interest. The need to develop nonintrusive techniques is apparent for all flow regimes, but it becomes of particular concern for the subsonic combustion flows so often of interest in thermophysics research. The volume contains scientific descriptions of the methods for making such measurements, primarily of gas temperature and pressure and particle size.

Published in 1984, 347 pp., 6×9, illus., $49.50 Mem., $69.50 List; ISBN 0-915928-86-8

TO ORDER WRITE: Publications Order Dept., AIAA, 1633 Broadway, New York, N.Y. 10019